JOC The Journal of Organic Chemistry

Article

pubs.acs.org/joc

Influence of Conjugation Axis on the Optical and Electronic Properties of Aryl-Substituted Benzobisoxazoles

Brian C. Tlach,[†] Aimée L. Tomlinson,[‡] Alden G. Ryno,[‡] Dawn D. Knoble,[†] Dana L. Drochner,[†] Kyle J. Krager, and Malika Jeffries-EL*[,†]

[†]Department of Chemistry, Iowa State University, Ames, Iowa 50010, United States

[‡]Department of Chemistry, University of North Georgia, Dahlonega, Georgia 30597, United States

Supporting Information

ABSTRACT: Six different 2,6-diethyl-4,8-diarylbenzo[1,2-*d*:4,5-*d*′]bis(oxazoles) and four different 2,4,6,8-tetraarylbenzobisoxazoles were synthesized in two steps: a Lewis acid catalyzed orthoester cyclization followed by a Suzuki or Stille cross-coupling with various arenes. The influence of aryl group substitution and/or conjugation axis variation on the optical and electronic properties of these benzobis(oxazole) (BBO) compounds was evaluated. Structural modifications could be used to alter the HOMO, LUMO, and band gap over a range of 1.0, 0.5, and 0.5 eV, respectively. However, depending on the location and identity of the substituent, the HOMO level can be altered without significantly impacting the LUMO level. This is supported by the calculated frontier molecular orbitals. Our results indicate that the FMOs and band gaps of benzobisoxazoles can be readily modified either jointly or individually.

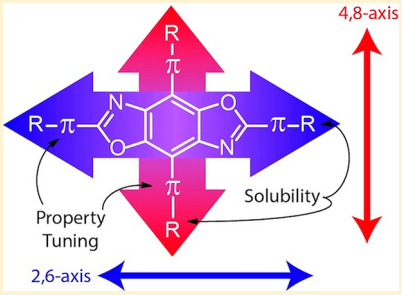

INTRODUCTION

During the past four decades, interest in the development of π-conjugated materials has increased due to their potential use as replacements for inorganic materials in a variety of semiconducting applications including field effect transistors (FETs),[1−5] organic light emitting diodes (OLEDs),[6−8] and photovoltaic cells (PVCs).[9−12] In addition to the ability to be processed from solution, organic semiconductors can be modified at the molecular level to optimize the optical and electronic properties of the materials for specific applications. Since the characteristics of π-conjugated systems are strongly influenced by the highest occupied molecular orbital (HOMO) and the lowest unoccupied molecular orbital (LUMO), synthetic strategies that can alter these parameters are of paramount importance. Unfortunately, most chemical modifications of π-conjugated materials result in changes in the position of both of the frontier molecular orbitals (FMOs). This is a result of the extensive delocalization of electrons within these systems, rendering selective modification of either the HOMO level or LUMO level difficult. One approach for independently tuning FMOs within π-conjugated materials is through the synthesis of two-dimensional molecules that feature two perpendicular π-conjugated linear "arms" connected through a central aromatic core.[13−23] These so-called "cruciforms" possess spatially segregated FMOs, enabling strategic tuning of either the LUMO or the HOMO by varying the nature of the substituents and their arrangement around the central molecule. Representative examples include benzobis(oxazole)-based cruciforms,[13−15] distyrylbis(arylethynyl)benzenes,[16−18] tetrakis(arylethynyl)benzenes,[19−22] and tetrastyrylbenzenes.[23]

Among the aforementioned examples, the benzo[1,2-*d*:4,5-*d*′]bis(oxazole) (BBO)-based cruciforms are particularly interesting, since these molecules have two different conjugation pathways: 2,6-conjugation through the oxazole rings and 4,8-conjugation through the central benzene ring (Scheme 1). Since one pathway encompasses heterocyclic rings, the optical and electronic properties can be altered as a function of the substitution pattern around the central benzene ring. Recently, our group[24,25] and that of Miljanić[13] have shown that the conjugation of BBOs is readily extended via Sonogashira cross-coupling reactions between 4,8-dibromoBBOs and various alkynes. The resulting materials have HOMO and LUMO levels that could readily be tuned by substitution. However, the synthesized cruciforms that were reported feature combinations of triple bonds between the arenes along the 4,8-axis and single bonds between the arenes along the 2,6-axis, so correlating optical and electronic properties to the conjugation pathway was not possible.[16,26,27] The Nuckolls group previously synthesized tetraarylBBO cruciforms; however, since their interest was in developing rigid molecules for self-assembled molecular electronics, the optical and electronic properties of these systems were not fully explored.[15,28]

In order to understand how different substitution patterns will affect the optical and electronic properties of larger BBO structures, we performed a more detailed structure−property relationship study. Modification of the aryl group has previously been used to vary properties through extension of the π system and inductive effects of their electron-donating or electron-withdrawing nature.[16,26−32] Furthermore, aryl substituents are

Received: April 24, 2013

dx.doi.org/10.1021/jo4007927 | J. Org. Chem. XXXX, XXX, XXX−XXX

Scheme 1. Proposed Sequential Functionalization of the 2,6- and 4,8-Axes of BBO

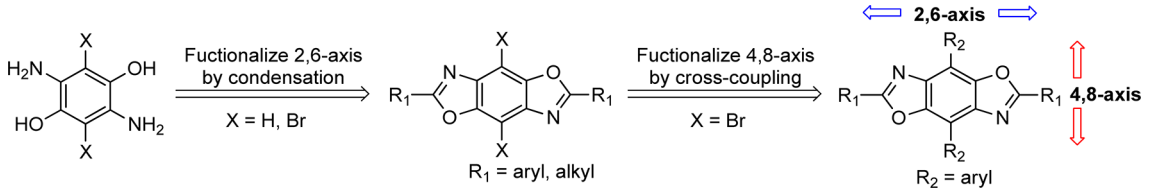

robust, are easily modified, and can be installed through a variety of methods. First, we evaluated the influence of different aryl groups at the 4- and 8-positions of the BBO moiety using a range of spectroscopic techniques along with computational modeling to gain further insight about the FMO shape and electron distribution. Then, we assessed the impact of conjugation pathway by comparing a pair of 2,6-diarylBBOs to the analogous 4,8-diarylBBOs. Finally, we compared four BBO cruciforms featuring two different aryl groups to study how properties change upon expanding to a two-dimensional π system. These structure−property studies provide basic insight on BBO behavior in two-dimensional π-systems as a function of aryl group selection and conjugation axis.

RESULTS AND DISCUSSION

Synthesis of 4,8-diarylBBOs. The synthesis of compounds **3**−**8** is shown in Scheme 2. Initially, we set out to synthesize

Scheme 2. Synthesis of 4,8-diaryl-2,6-diethylBBOs[a]

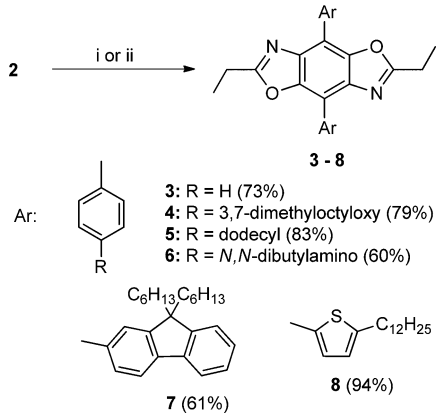

[a]Reaction conditions: (i, **3**−**7**) $Pd(dppf)Cl_2$, K_2CO_3, TBAB, boronic acid or ester, toluene/H_2O (10/1); (ii, **8**) $Pd_2(dba)_3$, $P(^oTolyl)_3$, 5-dodecyl-2-(trimethylstannyl)thiophene, toluene.

the 4,8-diarylBBOs using the Suzuki cross-coupling reaction of various arylboronic acids and 4,8-dibromo-2,6-dimethylBBO.[24] Suzuki coupling was chosen, as boronic acids and esters do not require the use of toxic reagents and are readily purified by standard techniques. Unfortunately, this approach gave low yields of 4,8-diarylBBOs. We hypothesized that the labile methyl protons were being deprotonated under the basic reaction conditions, resulting in undesirable side reactions. The Hegedus group previously decreased the reactivity of the 2,6-position of BBOs by substituting ethyl groups for methyl groups.[33] Therefore, we synthesized 2,6-diethyl BBOs **1** and **2** via the Lewis acid catalyzed condensation reaction between the corresponding diamino hydroquinone and triethyl orthopropionate, as shown in Scheme 3.[34−36] The Suzuki cross-coupling reaction of **2** and the appropriate boronic acids or esters afforded **3**−**7** in yields of 60−83%. Although arylboronic acids

Scheme 3. Synthesis of 2,6-diethylBBOs

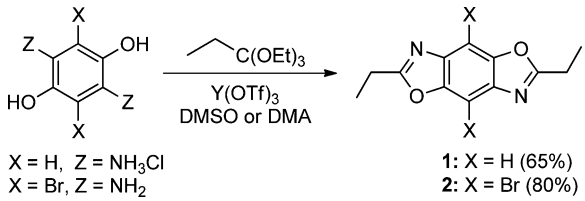

are easier and safer to synthesize, the facile protodeboronation that occurs with thien-2-ylboronic acids[37] required the use of a Stille cross-coupling for the synthesis of 4,8-bis(5-dodecylthien-2-yl)-2,6-diethylBBO **8**. To our knowledge, this is the first report of aryl−aryl cross-coupling of 4,8-dibromoBBOs.

Synthesis of 2,6-diarylBBOs. The synthetic approach for the 2,6-diarylBBOs is shown in Scheme 4, and the synthesis of the requisite orthoesters is shown in Scheme 5. We prepared 5-dodecyl-2-(triethoxymethyl)thiophene in one pot from 2-bromo-5-dodecylthiophene using the method reported by Tschitschibabin.[36,38] The synthesis of 4-dodecyl-1-(triethoxymethyl)benzene proved more difficult, as the Tschitschibabin method failed to yield the desired orthoester. In a search for an alternative approach, we found that aryl orthoesters have been prepared from trithio orthoester intermediates.[39,40] Since the corresponding aldehyde was more readily available, we decided to approach the synthesis of the trithio orthoester intermediate starting from 2-(4-bromophenyl)-1,3-dithiane. This decision proved beneficial, as the dithiane protecting group allowed for the addition of a solubilizing alkyl chain via a Kumada cross-coupling reaction, and the targeted orthoester was obtained in 84% yield. The 2,6-diarylBBOs **9** and **11** were obtained by the condensation of the corresponding orthoesters and 2,5-diamino-1,4-hydroquinone hydrochloride (DAHQ)[36,41] in yields of 73% and 65%, respectively. Due to their rigid-rod nature, compounds **9** and **11** had noticeably higher melting points and decreased solubility in comparison to their respective 4,8-diarylBBOs **5** and **7**.

Synthesis of 2,4,6,8-tetraarylBBOs. The synthetic approach for the 2,4,6,8-tetraarylBBOs is shown in Scheme 6. The Nuckolls group accomplished the synthesis of their tetraarylbenzo[1,2-*d*:4,5-*d*′]bis(oxazole) cruciforms via a double-Staudinger cyclization of substituted bis(azidoquinones).[15] Although the reactions occurred in good yields, in their strategy the substituents are introduced early in the reaction sequence. Thus, several steps are repeated to make different molecules. A more versatile approach is to first synthesize 2,6-diaryl-4,8-dibromoBBOs and then extend conjugation across the central benzene ring via cross-coupling chemistry. This approach allows for the synthesis of several BBOs using common intermediates. The condensation reaction of 3,6-diamino-2,5-dibromo-1,4-hydroquinone (Br-DAHQ) with 5-dodecyl-2-(triethoxymethyl)thiophene or 4-dodecyl-1-(triethoxymethyl)-

dx.doi.org/10.1021/jo4007927 | J. Org. Chem. XXXX, XXX, XXX−XXX

Scheme 4. Synthesis of 2,6-diarylBBOs

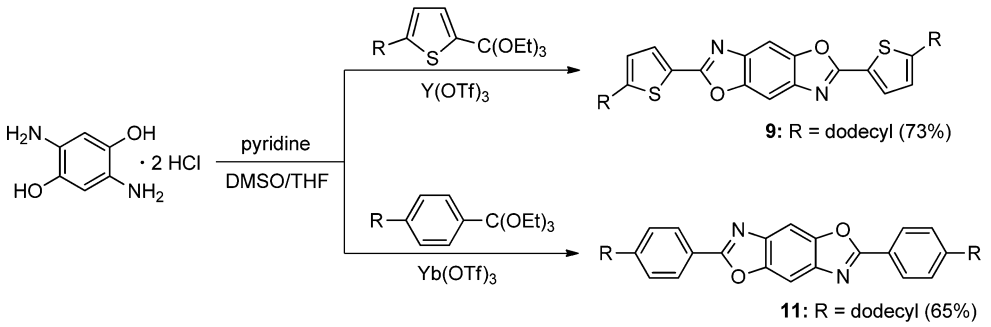

Scheme 5. Synthesis of Substituted Orthoesters

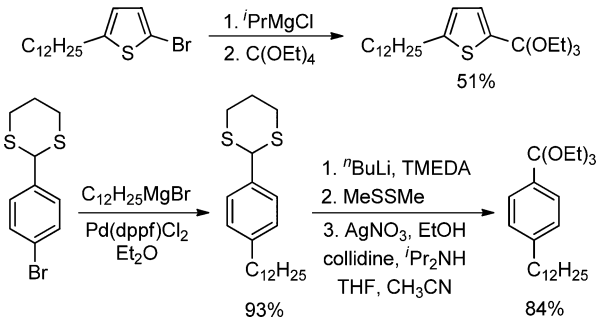

benzene afforded compounds **10** and **12** in yields of 75% and 68%, respectively. The subsequent cross-coupling of **10** and **12** with either 5-dodecyl-2-(trimethylstannyl)thiophene or (4-dodecylphenyl)boronic acid afforded cruciforms **13**–**16** in 60–94% yield. Purification of these compounds was easily accomplished by first passing through a short silica gel plug to remove polar impurities and residual catalyst followed by recrystallization from an appropriate solvent. The synthesized cruciforms were soluble in chlorinated solvents and characterized by ^{1}H NMR, ^{13}C NMR, and high-resolution mass spectrometry.

Spectroscopic and Electronic Characterization. *4,8-DiarylBBOs.* The HOMO levels of the BBOs were investigated using ultraviolet photoelectron spectroscopy (UPS), which provides an absolute determination of the HOMO level.[42−44] We elected to use UPS instead of electrochemistry, as many of the compounds were insoluble in acetonitrile and did not have a reduction cycle within the solvent window for the solvent/counterion blend used. The HOMO values of the BBOs ranged from −4.92 to −5.94 eV. The band gaps were estimated from the intersection of the absorption and emission spectra and

Scheme 6. Synthesis of BBO Cruciforms

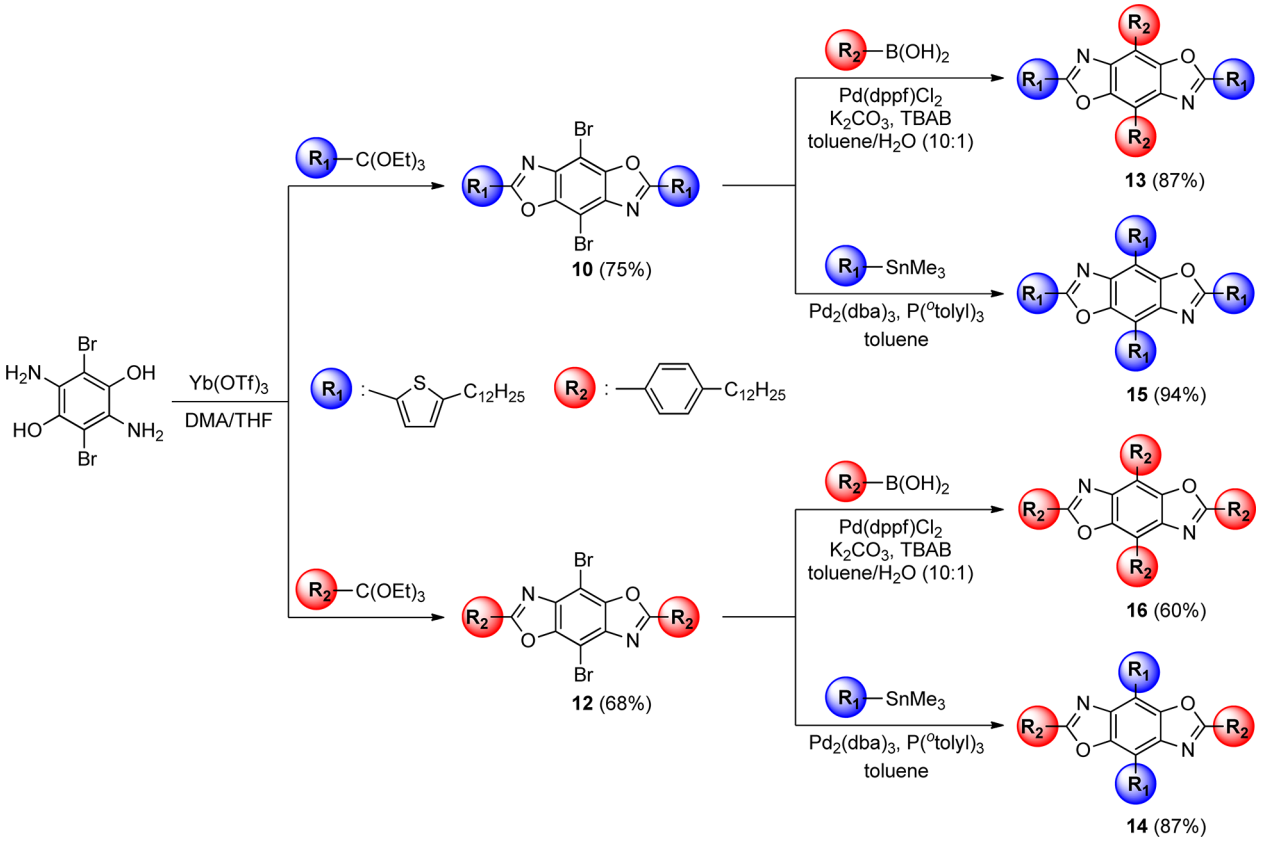

dx.doi.org/10.1021/jo4007927 | J. Org. Chem. XXXX, XXX, XXX−XXX

Table 1. Optical and Electronic Data for BBO Compounds

	λ_{max} (nm)[a]	λ_{em} (nm)[a]	ε (M^{-1} cm^{-1})[b]	ϕ[a,c]	HOMO (eV)[d]	LUMO (eV)[e]	E_g^{opt} (eV (nm))[f]
1	252	314	19200		−6.50	−2.3	4.2
3	314	372	42600	0.72	−5.94	−2.3	3.6
4	333	379	44700	0.80	−5.87	−2.5	3.4
5	320	381	46800	0.59	−5.96	−2.5	3.4
6	384	440	56400	0.81	−4.92	−2.0	3.0
7	358	404	72000	0.80	−5.98	−2.8	3.0
8	392	404	59000	0.34	−5.71	−2.6	3.1
9	369	396	78000	0.84	−5.51	−2.3	3.2
11	342	386	74900	0.98	−5.75	−2.3	3.4
13	380	416	85200	0.72	−5.78	−2.7	3.1
14	374	460	59600	0.28	−5.49	−2.7	2.8
15	395	448	67900	0.34	−5.29	−2.5	2.8
16	358	422	71500	0.74	−5.88	−2.7	3.2

[a]All measurements performed in THF. [b]Extinction coefficients based on absorbance at λ_{max}. [c]Relative Φ_{PL} values were measured using anthracene as a standard. [d]Measured by UPS. [e]Calculated using HOMO + E_g^{opt}. [f]Measured at the intersection of UV−vis and PL spectra.

ranged from 3.1 to 3.6 eV. The LUMO levels ranged from −2.0 to −2.5 eV and were calculated by adding the optical band gap to the HOMO values; thus, these values have a higher degree of uncertainty. These results are summarized in Table 1. The electronic properties of the BBOs varied substantially when aryl substituents were incorporated in the 4,8-axis. In general, the extent of the change was dependent on the electron-donating strength of the aryl substituent. BBO **3**, which bears a weakly donating phenyl substituent, has the deepest HOMO at −5.94 eV, whereas BBO **6**, which bears the most electron-rich substituent, has a HOMO level of −4.92 eV. BBO **6** also had the highest-lying LUMO (−2.0 eV), indicating that the incorporation of electron-rich *N,N*-dibutylaniline reduces the acceptor strength of the BBO. Overall, the deepest LUMO, −2.8 eV, was observed on the fluorene-substituted BBO **7**. This is most likely a result of the greater conjugation length, which increases the acceptor strength of the BBO in the absence of strong electron-donating groups.

The solution UV−vis absorption of the 4,8-diarylBBOs is shown in Figure 1, along with unsubstituted BBO **1**. All of the 4,8-diarylBBOs exhibit high-energy absorptions between 250 and 275 nm and a second more intense, lower energy absorption in the range of 312−392 nm. The magnitude of this shift varies as a function of the nature of the aryl substituent. Within the 4,8-diphenylBBO series, the maximum absorption (λ_{max}) increases with greater electron-donating strength of the phenyl substituent (H < alkyl < alkoxy < dialkylamino), and thus **3** absorbs at the shortest wavelength (314 nm) and **6** at the longest wavelength (384 nm). Similarly, BBO **8**, which bears thiophene rings, also has absorption at longer wavelengths, a result of the electron-rich nature of the substituents and the greater planarity of this molecule relative to the phenyl-substituted BBOs. Unlike the 4,8-diphenylBBOs, the main absorption of **8** has visible vibronic coupling likely due to a more planar structure, whereas the spectra of **3**−**7** all exhibit diminished vibronic detail due to the twisting between the aryl substituent and the BBO core.[45] Surprisingly, further extending the conjugation through the use of fluorene substituents did not display a large bathochromic shift in absorption. This is a result of the fluorene substituents being twisted out of plane due to steric interactions between the BBO core and the hydrogen atoms on fluorene.

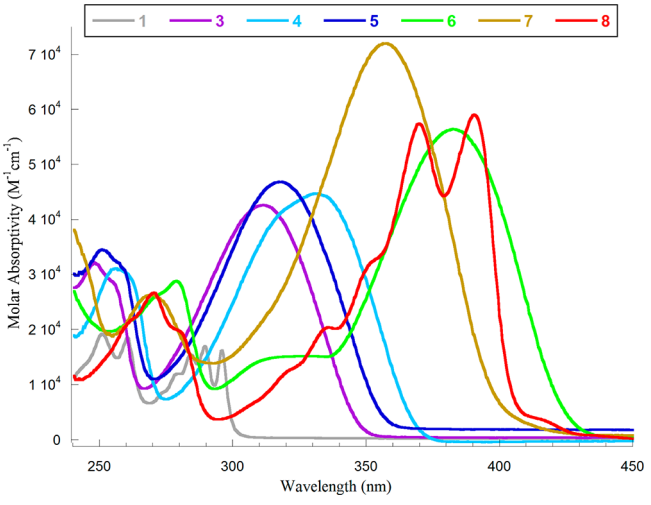

Figure 1. Solution UV−vis spectra of parent BBO **1** and 4,8-diarylBBOs **3**−**8**.

The PL spectra of BBOs **3**−**8** were obtained by exciting at their respective λ_{max} values and are shown in Figure S43 in the Supporting Information and summarized in Table 1. BBOs **3**−**8** show strong solution emission with similar profiles, each containing a main peak and a bathochromically shifted shoulder. The increased vibronic character in the PL spectra in comparison to the UV−vis spectra likely indicates that the excited state is more planar than the ground state.[46] The PL quantum yields (Φ_{PL}) of BBOs **3**−**8** were calculated using anthracene as a standard and an excitation wavelength at 325 nm. The incorporation of bulkier side groups or electron-donating groups results in an increase in Φ_{PL}, as seen previously in the literature.[30,47,48] Furthermore, thiophene substituents reduce Φ_{PL}, due to the heavy-atom effect of sulfur.

2,6-DiarylBBOs. The electronic properties of the 2,6-diarylBBOs are summarized in Table 1. On the basis of the data obtained from the 4,8-BBOs, we synthesized a pair of 2,6-analogues bearing alkylphenyl or alkylthienyl groups. These groups were selected as representative examples of weak and strong electron-donating substituents, respectively. We did not further evaluate the (dialkylamino)phenyl group, as it resulted in a high-lying HOMO on the 4,8-diarylBBO. Additionally, fluorene was not used due to its longer conjugation length, which would complicate comparisons. The position of the HOMO level exhibits a dependence on the nature of the aryl

dx.doi.org/10.1021/jo4007927 | J. Org. Chem. XXXX, XXX, XXX−XXX

group and is lowered by 0.24 eV when the aryl group is switched from a thiophene to a phenyl ring. This trend is the result of the increased donor strength of the thiophene in comparison to the phenyl substituent. Due to the uncertainty in the values, we cautiously state that the position of the LUMO level appears to be independent of the aryl group, as both **9** and **11** have similar LUMO levels. The band gaps vary proportionally to the HOMO as a result of the independent nature of the LUMO level with respect to the aryl substituent. Additionally, the UV−vis absorption spectra (Figure 2) are consistent with

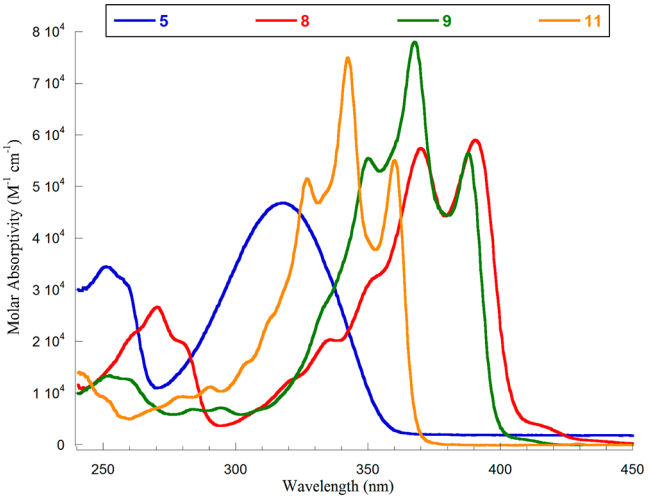

Figure 2. UV−vis spectra of 4,8-diarylBBOs **5** and **8** and the related 2,6-diarylBBOs **9** and **11**.

this finding, as the λ_{max} value of **9** is bathochromically shifted relative to that of **11**. PL spectra of **9** and **11** both exhibit vibronic coupling (Figure S43 in the Supporting Information). The Φ_{PL} values of the 2,6-diarylBBOs (0.84 for **9** and 0.98 for **11**) are also considerably higher than those for their corresponding 4,8-diarylBBOs (0.34 for **8** and 0.59 for **5**).

Importance of Substitution Axis. The observed differences in the shape of the UV−vis spectrum of the BBOs are most likely a result of varying degrees of planarity, which affects the conjugation length. The steric effects of the ortho hydrogens on the phenyl ring result in out-of-plane twisting along the 4,8-axis. This is supported by DFT calculations, which predict an out-of-plane twisting between 19 and 28° for **3**−**7**. In contrast, thiophene-substituted BBOs **8** and **9** are expected to be planar, regardless of which axis the ring is placed on. Phenyl-substituted BBO **11** is also planar, since the ring is placed at the 2,6-axis, minimizing the steric effects. Thus the 2,6-diarylBBOs **9** and **11** both have similar peak topographies, containing vibronic progression in the range of 1310−1410 cm^{-1}, which is characteristic of aromatic ring-stretching modes.[49,50] These features are seen to a small extent in **8** and are not observed in **5**. Further analysis of the absorption spectra reveals that moving the thienyl group from the 4,8-axis (**8**) to the 2,6-axis (**9**) results in a small bathochromic shift in absorption. However, switching the phenyl group from the 4,8-axis (**5**) to the 2,6-axis (**11**) produces a 22 nm bathochromic shift in λ_{max} and a slight reduction in peak width at half-maximum. This red shift is a result of both the longer conjugation pathway along the 2,6-axis and an increase in planarity. Compounds **5**, **8**, **9**, and **11** show similar PL spectra with Stokes shifts of 61, 12, 27, and 44 nm, respectively (Figure S43 in the Supporting Information). The HOMO level is raised by approximately 0.20 eV upon switching the substituents from the 4,8-axis to the 2,6-axis, i.e. **5** versus **11** or **8** versus **9**, suggesting that the HOMO preferentially aligns along the 4,8-axis. This decrease in stability was confirmed by the computational studies (Table S1 in the Supporting Information).

In order to further compare the effect of substituent type and location, a series of 2,4,6,8-tetraarylBBOs were synthesized and characterized. The Φ_{PL} values of cruciforms **13** (0.72) and **16** (0.74) are similar, while those of **14** (0.28) and **15** (0.34) were both significantly lower, which was expected, since Φ_{PL} commonly decreases with narrowing band gap. This has previously been observed in 1,4-bis(phenylethynyl)-2,5-bis(styryl)benzene cruciforms[17] and is a consequence of more accessible nonradiative processes in compounds with narrower band gaps.[51,52] Additionally, the λ_{em} value and vibronic detail in the PL spectra of the cruciforms display solvatochromism, in which there is a bathochromic shift in λ_{em} as the solvent polarity is increased (Figure 3 and Figure S46 in the Supporting

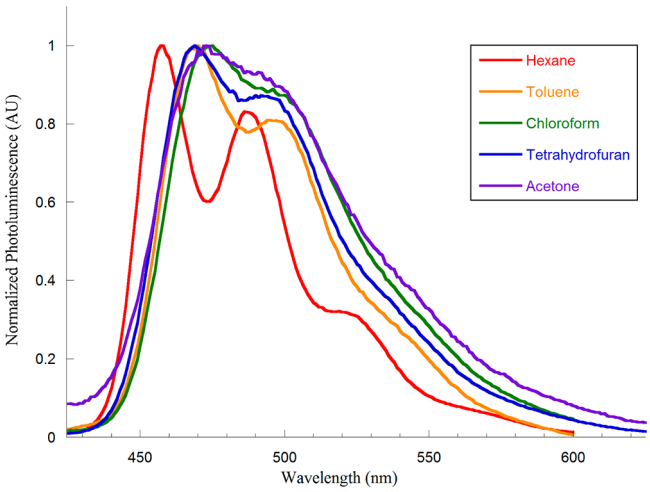

Figure 3. Solvatochromism effect of cruciform **15**.

Information). This is more apparent in cruciforms **14** and **15** than in **13** and **16**. The vibronic detail in the PL spectra decreased as the solvent polarity increased for all cruciforms except **13**. This type of behavior has previously been seen in cruciforms studied by Bunz and co-workers, who correlated the disappearance of vibronic character along with a bathochromic shift in λ_{em} of the PL spectra in highly polar solvents with intermolecular charge transfer (ICT) between the two arms of the cruciform.[17,53] Cruciforms **14** and **15** likely have more charge transfer between the two axes than cruciforms **13** and **16**. This is further substantiated by the observation of a lower energy shoulder in the UV−vis spectra and alignment of the FMOs in cruciforms **14** and **15** (vide infra).

An evaluation of cruciforms **15** and **16** demonstrates the influence of the aryl substituents on optoelectronic properties. Cruciform **16**, which bears phenyl substituents in all positions, has the lowest lying HOMO of all the cruciforms at −5.88 eV and the widest band gap at 3.2 eV. However, cruciform **15**, which bears electron-rich thiophenes in all positions, has the highest HOMO of all cruciforms at −5.29 eV and the smallest band gap at 2.8 eV. This is consistent with our observations (vide supra) that the addition of electron-donating groups at any position destabilizes the HOMO level. The impact of the

dx.doi.org/10.1021/jo4007927 | J. Org. Chem. XXXX, XXX, XXX−XXX

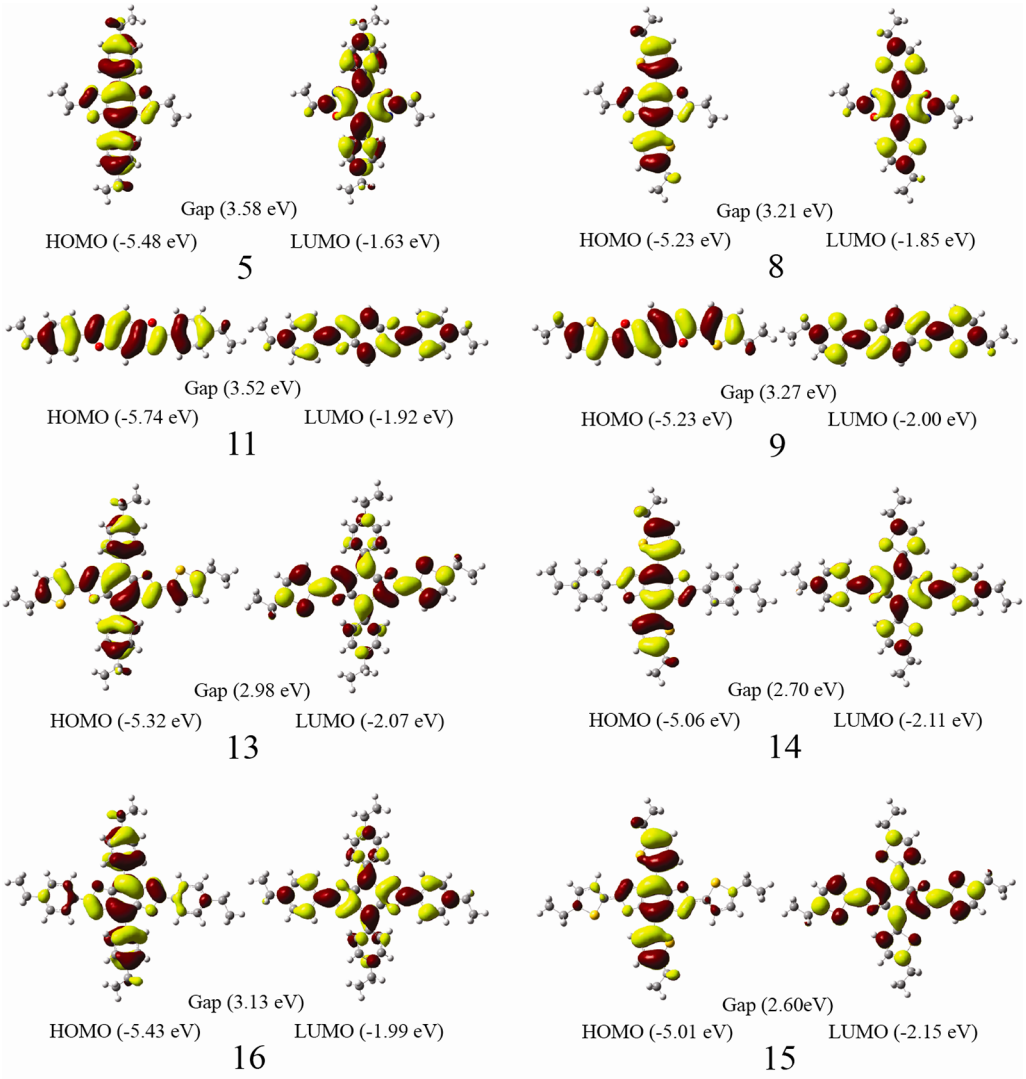

Figure 4. FMO diagrams of BBOs **5**, **8**, **9**, **11**, and **13**–**16**.

aryl group is substantiated by a comparison of the isomeric cruciforms **13** and **14**. Cruciform **14**, which has the strongly donating thiophene substituents along the 4,8-axis, has a HOMO that is nearly 0.3 eV higher and a band gap that is 0.2 eV narrower than that of **13**. This is likely the result of the difference in the planarity of the two structures along with the difference in the electron-donating behavior of the substituents. The origins of this difference may be further explained by comparing the FMO diagrams of the two compounds. Computational studies were carried out to gain further insight into the effect of structural modification by axis and/or aryl group variation. Optimized ground-state geometries were obtained through density functional theory (DFT) employing a B3LYP functional and a SVP basis set. The resulting FMO charge distributions of the optimized structures are shown in Figure 4, and the percent distributions along each axis are summarized in Table 2. The electron density is focused along the 2,6-axis in the LUMO of cruciforms **13**, **15**, and **16**, whereas it is distributed evenly across both axes of **14**. A comparison of the molecular orbital diagrams reveals significant differences in the HOMOs of **13** and **14**. In the case of **13**, the electron density is distributed throughout the entire structure, whereas in **14** approximately 96% of the electron density is along the

Table 2. Calculated Percent Electronic Distribution along Each Axis for the HOMO and LUMO of the BBO Cruciforms

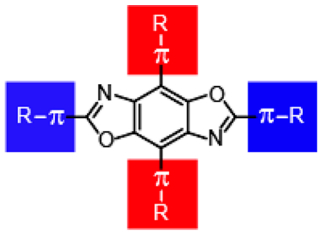

$$\%4,8-axis = \frac{\sum c^2_{4,8-axis}}{\sum c^2_{2,6-axis} + \sum c^2_{4,8-axis}} \qquad \%2,6-axis = \frac{\sum c^2_{2,6-axis}}{\sum c^2_{2,6-axis} + \sum c^2_{4,8-axis}}$$

	HOMO		LUMO	
	4,8-axis	2,6-axis	4,8-axis	2,6-axis
13	58.6	41.4	21.1	78.9
14	95.9	4.1	45.5	54.5
15	91.6	8.4	32.5	67.5
16	79.3	20.7	29.1	70.9

4,8-axis. This localization of the HOMO along the more electron-rich axis is consistent with observations made for other

dx.doi.org/10.1021/jo4007927 | J. Org. Chem. XXXX, XXX, XXX–XXX

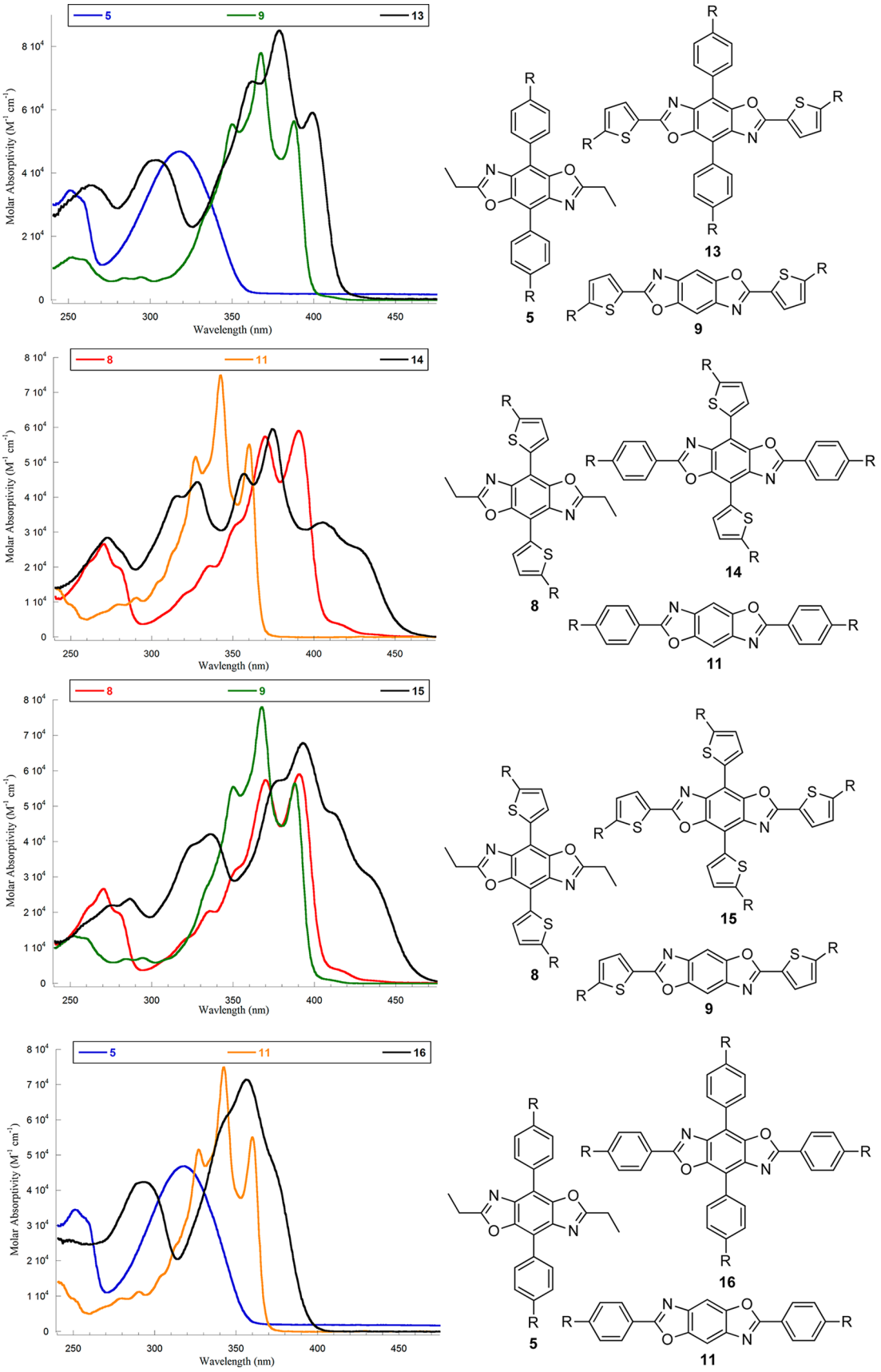

Figure 5. UV−vis spectra of BBO cruciforms **13**−**16** and their corresponding 1-D building blocks **5**, **8**, **9**, and **11** (left) and the corresponding structures where R = $C_{12}H_{25}$ (right).

dx.doi.org/10.1021/jo4007927 | J. Org. Chem. XXXX, XXX, XXX−XXX

cruciforms that contain donor−π−donor conjugation pathways.,[16,19,22,32,53−55] Interestingly, approximately 92% of the HOMO is also concentrated along the 4,8-axis in the tetrathiophene-substituted cruciform **15**, indicating that there is a preference for the HOMO to be aligned perpendicular to the benzobis(oxazole) ring system.[14]

A comparison of the BBO cruciforms to their 1-D building blocks gives further insight on the impact of aryl substituent location and nature. The UV−vis spectra of cruciforms **13**−**16** and their respective 1-D building blocks are shown in Figure 5, and the data are summarized in Table 1. Cruciform **13** has phenyl substituents along the 4,8-axis, analogous to the case for BBO **5**, and thiophene substituents along the 2,6-axis, analogous to the case for BBO **9**. The spectrum of **13** has high- and low-energy absorptions consistent with **5** and **9**, respectively. Additionally, the HOMO level of **13** is between that of **5** and **9**, indicating that **13** behaves as a hybrid of the two compounds. The FMOs show delocalization of electron density along the longest conjugation axis for **5** and **9**, whereas **13** shows delocalization throughout the molecule, consistent with our observations. Cruciform **14** has thiophene substituents along the 4,8-axis, analogous to the case for BBO **8**, and phenyl substituents along the 2,6-axis, analogous to the case for BBO **11**. The overall topography seen in the spectrum of **14** has absorptions consistent with **8** and **11**. However, the spectrum of **14** is significantly broader and has an additional low-energy peak around 412 nm, suggesting that ICT is occurring.[22,56] As a result, the HOMO level of **14** is higher than those of **8** and **11**. The fact that the band gap of **14** is smaller than that of its structural isomer **13** is further evidence of the importance of aryl substituent placement. The FMO diagram of **14** shows that there is a large amount of electron density localized along the 4,8-axis in the HOMO, providing a suitable environment for charge transfer. These results were somewhat contradictory to those seen for similar 2,6-diaryl-4,8-bis(arylethynyl)BBO cruciforms, in which the HOMO, in some cases, is fully localized along the 2,6-axis. In these tetraarylBBOs, full axial "inversion" of the HOMOs and LUMOs does not appear to be prompted by exchanging the aryl groups.[14] However, switching the aryl substituents does appear to have a significant effect on the extent of delocalization in the FMOs.

Cruciform **15** has thiophene substituents along the 4,8- and 2,6-axes, analogous to the cases for BBO **8** and BBO **9**, respectively. The spectrum of **15** is broad and lacking in structural detail; thus, direct comparisons to **8** and **9** are unclear. Similarly to **14**, there is significant broadening and the appearance of a lower energy shoulder in the spectrum of **15**, which is indicative of ICT. Furthermore, the larger Stokes shift and greater influence of solvent polarity on the λ_{em} values of **14** and **15** are also indicative of ICT. Collectively, the higher HOMO, narrower band gap, and FMOs of **14** and **15** support the notion that charge transfer is favorable when the 4,8-axis is substituted with thiophene.

Cruciform **16** has phenyl substituents along the 4,8- and 2,6-axes, analogous to the cases for BBO **5** and BBO **11**, respectively. As seen in cruciform **15**, the spectrum of **16** is also broad and lacking in structural detail; thus, direct comparisons to **5** and **11** are indeterminate. The diminished vibronic detail in **16**, and to a lesser extent in **13**, is likely a result of the more nonplanar structures of these cruciforms in comparison to **14** and **15** (vide supra). This trend also indicates that changes in the spectral topography may be related to the symmetry of these molecules. Of all the cruciforms in this study, **16** has the lowest HOMO and widest band gap. This is a result of a decrease in electron-donating strength and conjugation caused by the phenyl substituents on the 4,8-axis. The FMOs show a slight localization of electron density along the 4,8-axis in the HOMO and the 2,6-axis in the LUMO of **16**, consistent with our observations in the other cruciforms.

CONCLUSIONS

A series of related 4,8-diarylBBOs, 2,6-diarylBBOs, and 2,4,6,8-tetraarylBBO cruciforms were readily synthesized in a few high-yielding steps. It was observed that the optical and electronic properties of these molecules are dependent on both the electronic nature of the aryl substituent and its location. For linear molecules, as the electron-donating strength of the substituent was increased, the HOMO levels of the BBOs were raised regardless of axis. Additionally, BBOs with an electron-donating group along the 4,8-axis had lower lying HOMO levels than the analogous 2,6-BBOs. On the other hand, the LUMO levels for the related linear BBOs appeared to be unaffected by structural modifications. Similarly, with the mixed cruciforms placing the electron-donating group along the 4,8-axis resulted in a higher HOMO in comparison to that obtained when the substituent was placed on the 2,6-axis. Changing the location of the substituent impacted the LUMO levels for the cruciforms, whereas the band gaps remained unaffected. Collectively, the UV−vis, PL, and DFT results indicate that the FMOs and band gaps of benzobisoxazoles can be readily modified either jointly or independently of each other. This result is of significance in the design of new materials for use in a range of organic semiconducting applications. Work is ongoing in our laboratories to develop new two-dimensional oligomers and conjugated polymers.

EXPERIMENTAL SECTION

General Methods. Nuclear magnetic resonance (NMR) experiments were carried out in $CDCl_3$ at 400 MHz (^{1}H) or 100 MHz (^{13}C). ^{1}H NMR spectra are internally referenced to the residually protonated solvent peak (7.26 ppm), and ^{13}C NMR spectra are referenced to the central carbon peak (77.16 ppm) of $CDCl_3$. In all spectra, chemical shifts are given in δ relative to tetramethylsilane. Coupling constants are reported in hertz (Hz). High-resolution mass spectra were recorded on a double-focusing magnetic sector mass spectrometer using EI, ESI, or APCI. Melting points were obtained on a melting point apparatus with 260 °C upper limit and are uncorrected. All UV−vis and fluorescence spectra were obtained using THF solutions unless otherwise noted. Relative solution fluorescence quantum yields were obtained using anthracene (Φ_{PL} = 0.27 in ethanol)[57] as a standard with excitation at 325 nm. Ultraviolet photoelectron spectroscopy (UPS) measurements were performed on sample films spun from $CHCl_3$. DAHQ,[35] Br-DAHQ,[58] 1-bromo-4-(3,7-dimethyloctyloxy)benzene,[58] 4-dodecyl-1-iodobenzene,[58] 4-dodecylphenylboronic acid,[59] 2-bromo-9,9-dihexylfluorene,[60] 2-(4,4,5,5-tetramethyl-1,3,2-dioxaborolan-2-yl)-9,9-dihexylfluorene,[61] *N*,*N*-dibutylaniline,[62,63] 4-bromo-*N*,*N*-dibutylaniline,[63] 4-(dibutylamino)phenylboronic acid,[64] 2-bromo-5-dodecanoylthiophene,[65] 2-bromo-5-dodecylthiophene,[65,66] 5-dodecyl-2-(trimethylstannyl)thiophene,[67] and 2-(4-bromophenyl)-1,3-dithiane[68] were synthesized according to literature procedures.

2,6-Diethylbenzo[1,2-*d*;4,5-*d*′]bis(oxazole) (1). A dry round-bottom flask was placed under an argon atmosphere and charged with 0.054 g (0.05 mmol) $Y(OTf)_3$ and 1.06 g (6.00 mmol) of triethyl orthopropionate. The flask was fitted with a dry addition funnel and heated to 55 °C with stirring. In the addition funnel, 0.43 g (2.00 mmol) of DAHQ was dissolved in 0.33 g (4.20 mmol) of pyridine and 2 mL of DMSO and the solution added dropwise to the flask. The mixture was stirred at 55 °C for 2 h and then cooled to room temperature and diluted with water. The resulting precipitate was

dx.doi.org/10.1021/jo4007927 | J. Org. Chem. XXXX, XXX, XXX−XXX

collected by filtration and washed with water. The crude product was purified by recrystallization from hexanes to give white needles (0.28 g, 65% yield): mp 95−97 °C; ^{1}H NMR (400 MHz, $CDCl_3$) δ 1.45 (6H, t, J = 8 Hz) 2.96 (4H, q, J = 8 Hz), 7.70 (2H, s, J = 8 Hz); ^{13}C NMR (100 MHz, $CDCl_3$) δ11.0, 22.5, 100.5, 139.2, 148.3, 169.4; HRMS (ESI) m/z calcd for $C_{12}H_{13}N_2O_2$ 217.0972 $[M + H]^+$, found 217.0972.

4,8-Dibromo-2,6-diethylbenzo[1,2-*d*;4,5-*d*′]bis(oxazole) (2). A dry round-bottom flask was placed under an argon atmosphere and charged with 0.52 g (0.98 mmol) of $Y(OTf)_3$, 21 mL of DMA, and 10.3 g (58.5 mmol) of triethyl orthopropionate. The mixture was heated to 55 °C with stirring, and 5.81 g (19.5 mmol) freshly prepared Br-DAHQ was added portionwise over 45 min. The reaction mixture was stirred at 55 °C for 2 h and then cooled to room temperature and diluted with water. The resulting precipitate was collected by filtration and rinsed with water and ethanol. The crude product was further purified by recrystallization from 1/1 chloroform/ethanol to give small white needles (5.85 g, 80% yield): mp 216−218 °C; ^{1}H NMR (400 MHz, $CDCl_3$) δ 1.50 (6H, t, J = 8 Hz) 3.06 (4H, q, J = 8 Hz); ^{13}C NMR (100 MHz, $CDCl_3$) δ 11.3, 22.8, 91.4, 138.6, 146.7, 170.0; HRMS (ESI) m/z calcd for $C_{12}H_{11}Br_2N_2O_2$ 372.9182 $[M + H]^+$, found 372.9197.

4,8-Diphenyl-2,6-diethylbenzo[1,2-*d*;4,5-*d*′]bis(oxazole) (3). A two-neck round-bottom flask was charged with 0.37 g (1.00 mmol) of **2**, 0.10 g (1.00 mmol) of tetrabutylammonium bromide (TBAB), and 0.33 g (3.0 mmol) of phenylboronic acid. The flask was equipped with a reflux condenser and placed under an argon atmosphere. A 25 mL portion of deoxygenated toluene was added followed by 2 mL of deoxygenated 3 M aqueous K_2CO_3. The mixture was further deoxygenated for 10 min, then 0.036 g (0.05 mmol) of $Pd(dppf)Cl_2$ was added, and the reaction mixture was heated to reflux with stirring under an argon atmosphere for 36 h. The mixture was cooled to room temperature and diluted with toluene, and the layers were separated. The organic layer was washed with 1 M HCl, H_2O, and brine and dried over $MgSO_4$. The solution was filtered and the solvent removed in vacuo. The crude product was taken up in hot hexanes and filtered, and the solvent was removed in vacuo. The product was further purified by recrystallization from acetone to give white needles (0.27 g, 73% yield): mp 178−179 °C; ^{1}H NMR (400 MHz, $CDCl_3$) δ 1.50 (6H, q, J = 8 Hz), 3.05 (4H, t, J = 8 Hz), 7.45 (2H, m), 7.58 (4H, m), 8.23 (4H, d, J = 8 Hz); ^{13}C NMR (100 MHz, $CDCl_3$) δ 11.5, 22.8, 114.1, 128.3, 128.8, 130.2, 132.7, 137.2, 146.2, 169.0; HRMS (ESI) m/z calcd for $C_{24}H_{21}N_2O_2$ 369.1598 $[M + H]^+$, found 369.1603.

4,8-Bis(4-((3,7-dimethyloctyl)oxy)phenyl)-2,6-diethylbenzo-[1,2-*d*;4,5-*d*′]bis(oxazole) (4). *(4-((3,7-Dimethyloctyl)oxy)phenyl)-boronic Acid.* A dry, two-neck round-bottom flask was placed under an argon atmosphere and charged with 300 mL of dry THF and 9.88 g (30.0 mmol) of 4-((3,7-dimethyloctyl)oxy)-1-bromobenzene. The solution was cooled to −78 °C in a dry ice/acetone bath, 15.0 mL of ^{n}BuLi (2.5 M in hexanes) was added dropwise, and the mixture was stirred at −78 °C for 1 h. A 9.35 g (90.0 mmol) amount of $B(OMe)_3$ was added dropwise to the solution, and the mixture was stirred at −78 °C for 1 h and warmed to room temperature over 3 h. The reaction was quenched with 2 M HCl (25 mL), and the mixture was extracted with diethyl ether. The combined organic layers were washed with water and brine and dried over $MgSO_4$. The solution was filtered and the solvent removed in vacuo. The resulting solid was dried under vacuum overnight to give an off-white paste that was used without further purification (2.90 g, 35% yield): ^{1}H NMR (400 MHz, $CDCl_3$) δ 0.90 (6H, d, J = 8 Hz), 1.00 (3H, d, J = 8 Hz), 1.21−1.88 (10H, comp), 4.09 (2H, m), 7.02 (2H, d, J = 8 Hz), 8.17 (2H, d, J = 8 Hz); ^{13}C NMR (100 MHz, $CDCl_3$) δ 19.9, 22.9, 23.0, 24.9, 28.2, 36.4, 36.5, 37.5, 39.5, 66.4, 114.1, 115.7, 137.6, 162.9.

4,8-Bis(4-((3,7-dimethyloctyl)oxy)phenyl)-2,6-diethylbenzo[1,2-d;4,5-d′]bis(oxazole) (4). This compound was prepared analogously to BBO **3** from BBO **2** (1.00 mmol) and (4-((3,7-dimethyloctyl)oxy)-phenyl)boronic acid. The product was purified by column chromatography with hexanes/chloroform as eluent (3/1 gradient to 1/3) followed by recrystallization from hexanes to give a white powder (0.54 g, 79% yield): mp 74−76 °C. ^{1}H NMR (400 MHz, $CDCl_3$) δ 0.91 (12H, d, J = 8 Hz), 0.98 (6H, d, J = 8 Hz), 1.2−1.37 (12H, comp), 1.52 (6H, t, J = 8 Hz), 1.75−1.92 (8H, comp), 3.04 (4H, q, J = 8 Hz), 4.11 (4H, m), 7.11 (4H, d, J = 8 Hz, 8.21 (4H, d, J = 8 Hz); ^{13}C NMR (100 MHz, $CDCl_3$) δ 11.5, 19.9, 22.79, 22.84, 23.0, 25.0, 28.2, 30.1, 36.4, 37.5, 39.5, 66.5, 113.2, 114.8, 125.1, 131.4, 136.8, 146.0, 159.1, 168.6; HRMS (ESI) m/z calcd for $C_{44}H_{61}N_2O_4$ 681.4626 $[M + H]^+$, found 681.4636.

4,8-Bis(4-dodecylphenyl)-2,6-diethylbenzo[1,2-*d*;4,5-*d*′]bis-(oxazole) (5). This compound was prepared analogously to BBO **3** from BBO **2** (1.00 mmol) and (4-dodecylphenyl)boronic acid. The product was purified by column chromatography with hexanes/chloroform as eluent (3/1 gradient to 1/3) followed by recrystallization from hexanes to give a white powder (0.59 g, 83% yield): mp 103−105 °C; ^{1}H NMR (400 MHz, $CDCl_3$) δ 0.89 (6H, t, J = 8 Hz, 1.28 (36H, comp), 1.47 (6H, t, J = 8 Hz), 1.70 (4H, m), 2.70 (4H, t, J = 8 Hz), 3.03 (4H, q, J = 8 Hz), 7.39 (4H, d, J = 8 Hz), 8.15 (4H, d, J = 8 Hz); ^{13}C NMR (100 MHz, $CDCl_3$) δ 11.6, 14.4, 22.8, 22.9, 29.6, 29.7, 29.82, 29.87, 29.89, 29.94, 31.7, 32.2, 36.2, 113.9, 128.9, 130.0, 137.0, 143.2, 146.2, 168.8; HRMS (ESI) m/z calcd for $C_{48}H_{69}N_2O_2$ 705.5354 $[M + H]^+$, found 705.5372.

4,8-Bis(4-(dibutylamino)phenyl)-2,6-diethylbenzo[1,2-*d*;4,5-*d*′]bis(oxazole) (6). This compound was prepared analogously to BBO **3** from BBO **2** (1.00 mmol) and (4-(dibutylamino)phenyl)-boronic acid. The product was purified by column chromatography with 1/1 hexanes/toluene as eluent followed by recrystallization from acetone to give small yellow needles (0.26 g, 60% yield): mp 103−105 °C. ^{1}H NMR (400 MHz, $CDCl_3$) δ 0.99 (6H, t, J = 8 Hz, 1.40 (4H, p, J = 8 Hz), 1.51 (4H, t, J = 8 Hz), 1.65 (4H, m), 3.04 (4H, q, J = 8 Hz), 3.36 (4H, t, J = 8 Hz), 6.82 (4H, d, J = 8 Hz), 8.16 (4H, d, J = 8 Hz). ^{13}C NMR (100 MHz, $CDCl_3$) δ 11.7, 14.3, 20.6, 22.8, 29.8, 51.0, 111.7, 113.0, 119.7, 131.0, 136.5, 146.0, 147.8, 168.0; HRMS (ESI) m/z calcd for $C_{40}H_{55}N_4O_2$ 623.4320 $[M + H]^+$, found 623.4302.

4,8-Bis(9,9-dihexylfluoren-2-yl)-2,6-diethylbenzo[1,2-*d*;4,5-*d*′]bis(oxazole) (7). This compound was prepared analogously to BBO **3** from BBO **2** (1.00 mmol) and 2-(4,4,5,5-tetramethyl-1,3,2-dioxaborolan-2-yl)-9,9-dihexylfluorene. The product was purified by column chromatography with hexanes/$CHCl_3$ as eluent (3/1 gradient to 1/1) followed by recrystallization from hexanes to give a white solid (0.37 g, 61% yield): mp 157−160 °C; ^{1}H NMR (400 MHz, $CDCl_3$) δ 0.78 (12H, t, J = 8 Hz), 0.86 (8H, m), 1.09−1.17 (24H, comp), 1.55 (6H, t, J = 8 Hz), 2.06 (8H, m), 3.09 (4H, q, J = 8 Hz), 7.33−7.42 (6H, comp), 7.79 (2H, d, J = 8 Hz), 7.91 (2H, d, J = 8 Hz), 8.25 (2H, s), 8.29 (2H, d, J = 8 Hz); ^{13}C NMR (100 MHz, $CDCl_3$) δ 11.3, 13.2, 22.86, 22.90, 24.2, 30.1, 31.8, 40.7, 55.3, 114.6, 120.0, 120.1, 123.1, 125.0, 127.0, 127.4, 129.0, 131.4, 137.2, 141.0, 141.1, 146.4, 150.9, 152.6; HRMS (ESI) m/z calcd for $C_{62}H_{77}N_2O_2$ 881.5980 $[M + H]^+$, found 881.5979.

4,8-Bis(5-dodecylthien-2-yl)-2,6-diethylbenzo[1,2-*d*;4,5-*d*′]-bis(oxazole) (8). A dry, two-neck round-bottom flask was fitted with a reflux condenser, placed under an argon atmosphere, and charged with 0.28 g (0.75 mmol) of **2**, 0.70 g (1.67 mmol) of 5-dodecyl-2-(trimethylstannyl)thiophene, and 15 mL of dry, deoxygenated toluene. The mixture was further deoxygenated for 10 min and then charged with 9.1 mg (0.03 mmol) of $P(^o\text{tolyl})_3$ and 13.7 mg (0.015 mmol) of $Pd_2(dba)_3$. The reaction mixture was heated to reflux with stirring under an argon atmosphere for 24 h, cooled to room temperature, and concentrated in vacuo. The crude mixture was dissolved in CH_2Cl_2 and passed through a pad of silica gel with CH_2Cl_2 as eluent, and the solution was concentrated in vacuo. The product was further purified by recrystallization from hexane to give small light yellow needles (0.51 g, 94% yield): mp 97−99 °C; ^{1}H NMR (400 MHz, $CDCl_3$) δ 0.88 (6H, t, J = 8 Hz), 1.26−1.43 (36H, comp), 1.56 (6H, t, J = 8 Hz), 1.77 (4H, m), 2.91 (4H, t, J = 8 Hz), 3.11 (4H, q, J = 8 Hz), 6.90 (2H, d, J = 4 Hz), 8.11 (2H,d, J = 8 Hz); ^{13}C NMR (100 MHz, $CDCl_3$) δ 11.4, 14.4, 22.89, 22.92, 29.4, 29.58, 29.64, 29.82, 29.87, 29.90, 30.4, 32.0, 32.1, 107.8, 124.8, 128.8, 131.9, 135.4, 144.5, 148.2, 168.4; HRMS (ESI) m/z calcd for $C_{44}H_{65}N_2O_2S_2$ 717.4482 $[M + H]^+$, found 717.4488.

5-Dodecyl-2-(triethoxymethyl)thiophene. A dry, three-neck round-bottom flask was equipped with a reflux condenser and placed

dx.doi.org/10.1021/jo4007927 | J. Org. Chem. XXXX, XXX, XXX−XXX

under an argon atmosphere. The flask was charged with 8.28 g (25.0 mmol) of 2-bromo-5-dodecylthiophene and 25 mL of dry diethyl ether. A 13.8 mL (27.5 mmol) amount of ^{i}PrMgCl (2.0 M in ether) was added dropwise, and the reaction mixture was heated to reflux with stirring for 24 h and then cooled to room temperature. A solution of 5.53 g (28.8 mmol) of tetraethyl orthocarbonate in 20 mL of dry diethyl ether was added dropwise and the mixture heated to reflux with stirring overnight. The mixture was cooled to room temperature and poured into a saturated aqueous solution of NH_4Cl. The layers were separated, and the aqueous layer was extracted with ether. The combined organic layers washed with water and brine and dried over $MgSO_4$. The solution was filtered and the solvent removed in vacuo. The low-boiling impurities were removed by vacuum distillation, and the resulting red oil was used without further purification (5.05 g, 51% yield): ^{1}H NMR (400 MHz, $CDCl_3$) δ 0.89 (3H, t, J = 8 Hz), 1.20 (9H, t, J = 8 Hz), 1.21−1.40 (18H, comp), 1.67 (2H, m), 2.77 (3H, t, J = 8 Hz), 3.46 (2H, q, J = 8 Hz), 6.64 (1H, d, J = 4 Hz), 6.98 (1H, d, J = 4 Hz); ^{13}C NMR (100 MHz, $CDCl_3$) 14.3, 15.1, 22.9, 29.3, 29.5, 29.6, 29.84, 29.86, 29.88, 30.4, 31.7, 32.1, 58.1, 113.2, 123.4, 126.7, 139.0, 147.0; HRMS (ESI) m/z calcd for $C_{23}H_{42}NaO_3S$ 421.2747 [M + Na]$^+$, found 421.2753.

2,6-Bis(5-dodecylthien-2-yl)benzo[1,2-*d*;4,5-*d*′]bis(oxazole) (9). A dry Schlenk flask was placed under an argon atmosphere and charged with 1.59 g (4.00 mmol) of 5-dodecyl-2-(triethoxymethyl)-thiophene, 27 mg (0.050 mmol) of $Y(OTf)_3$, and 1 mL of THF. The solution was deoxygenated for 20 min and then heated to 55 °C with stirring. Concurrently, a dry 5 mL pear-bottom flask was place under an argon atmosphere, 1 mL of DMSO was added, and the flask and contents were deoxygenated for 20 min. The pear-bottom flask was charged with 0.21 g (1.00 mmol) of DAHQ and 0.164 g (2.10 mmol) of pyridine, and the resulting solution was added dropwise to the THF solution at 55 °C. After 3 h, the reaction mixture was diluted with 3 mL of THF and stirred at 55 °C overnight. The mixture was cooled to room temperature and diluted with methanol. The resulting precipitate was filtered and rinsed with methanol. The product was purified by recrystallization from $CHCl_3$ to give a yellow solid (0.48 g, 73% yield): mp 190−192 °C; ^{1}H NMR (400 MHz, $CDCl_3$) δ 0.89 (6H, t, J = 8 Hz), 1.27−1.41 (36H, comp), 1.75 (4H, p, J = 8 Hz), 2.90 (4H, t, J = 8 Hz), 6.89 (2H, d, J = 4 Hz), 7.75 (2H, d, J = 4 Hz), 7.80 (2H, s); ^{13}C NMR (100 MHz, $CDCl_3$) δ 14.3, 22.9, 29.3, 29.6, 29.76, 29.85, 29.89, 30.7, 31.7, 32.2, 100.6, 125.9, 127.0, 130.4, 140.5, 148.6, 152.6, 160.6; HRMS (ESI) m/z calcd for $C_{38}H_{57}N_2O_2S_2$ 661.3832 [M + H]$^+$, found 661.3837.

4,8-Dibromo-2,6-bis(5-dodecylthien-2-yl)benzo[1,2-*d*;3,4-*d*′]bis(oxazole) (10). A dry Schlenk flask was placed under an argon atmosphere and charged with 4.78 g (12.0 mmol) of 5-dodecyl-2-(triethoxymethyl)thiophene, 5 mL of dry DMA, and 5 mL of dry THF. The mixture was deoxygenated for 20 min, 0.12 g (0.20 mmol) of $Yb(OTf)_3$ was added, and the mixture was heated to 55 °C. A 1.19 g (4.00 mmol) amount of of freshly prepared Br-DAHQ was added portionwise, and the reaction mixture was diluted with 5 mL of THF after 3 h and stirred at 55 °C overnight. The mixture was cooled to room temperature and diluted with methanol. The resulting precipitate was filtered and rinsed with methanol. The product was purified by recrystallization from $CHCl_3$ to give pale yellow needles (2.45 g, 75% yield): mp 190−192 °C; ^{1}H NMR (400 MHz, $CDCl_3$) δ 0.90 (6H, t, J = 8 Hz), 1.29−1.43 (36H, comp), 1.77 (4H, p, J = 8 Hz), 2.92 (4H, t, J = 8 Hz), 6.90 (2H, d, J = 8 Hz), 7.87 (2H, d, J = 4 Hz); ^{13}C NMR (100 MHz, $CDCl_3$) δ 14.3, 22.9, 29.3, 29.55, 29.57, 29.7, 29.85, 29.86, 29.89, 30.7, 31.6, 32.2, 91.3, 125.9, 126.0, 131.8, 139.8, 146.9, 153.9, 160.7; HRMS (ESI) m/z calcd for $C_{40}H_{55}Br_2N_2O_2S_2$ 817.2046 [M + H]$^+$, found 817.2066.

4-Dodecyl-1-(triethoxymethyl)benzene. *2-(4-Dodecylphenyl)-1,3-dithiane.* A dry three-neck round-bottom flask was equipped with a reflux condenser and placed under an argon atmosphere. The flask was charged with 7.05 g (25.6 mmol) of 2-(4-bromophenyl)-1,3-dithiane, 60 mL of dry, deoxygenated ether, and 0.21 g (0.256 mmol) of $Pd(dppf)Cl_2{\cdot}CH_2Cl_2$. The flask was placed in an ice/water bath, and 30.7 mL (30.7 mmol) of dodecylmagnesium bromide (1.0 M in ether) was added dropwise. The mixture was warmed to room temperature and then heated to reflux with stirring overnight. The mixture was cooled to room temperature and poured into cold 1 M HCl, and the layers were separated. The aqueous layer was extracted with ether, and the combined organic layers were washed with 1 M HCl, water, and brine and dried over $MgSO_4$. The solution was filtered, and the solvent was removed in vacuo. The crude product was purified by recrystallization from isopropyl alcohol to give ivory-colored needles (9.32 g, 93% yield): mp 52−54 °C; ^{1}H NMR (400 MHz, $CDCl_3$) δ 0.88 (3H, t, J = 8 Hz), 1.25−1.35 (18H, comp), 1.60 (2H, p, J = 8 Hz), 1.92 (1H, m), 2.16 (1H, m), 2.57 (2H, t, J = 8 Hz), 2.90 (2H, dt), 3.06 (2H, td), 5.15 (1H, s), 7.14 (2H, d, J = 8 Hz), 7.36 (2H, d, J = 8 Hz); ^{13}C NMR (100 MHz, $CDCl_3$) δ 14.3, 22.8, 25.3, 29.49, 29.50, 29.65, 29.73, 29.78, 29.8, 31.5, 32.1, 32.3, 51.4, 127.7, 128.9, 136.4, 143.5; HRMS (APCI) m/z calcd for $C_{22}H_{37}S_2$ 365.2331 [M + H]$^+$, found 365.2341.

4-Dodecyl-1-(triethoxymethyl)benzene. A dry, two-neck round-bottom flask was placed under an argon atmosphere and charged with 1.82 g (5.00 mmol) of 2-(4-dodecylphenyl)-1,3-dithiane, 1.16 g (10.0 mmol) of TMEDA, and 50 mL of dry THF. The flask was cooled to −78 °C in a dry ice/acetone bath, and 2.2 mL (5.5 mmol) of ^{n}BuLi (2.5 M in hexane) was added dropwise. The flask was stirred for 1 h at −78 °C, and 0.55 mL (6.00 mmol) of dimethyl disulfide was added in one portion. The mixture was stirred for 30 min at −78 °C and warmed to room temperature over 3 h. The reaction mixture was quenched with water and extracted with ether. The combined organic layers were washed with water and brine and dried over Na_2SO_4. The solution was filtered and concentrated in vacuo. The remaining residue was dried under vacuum with stirring overnight. The flask was back-filled with argon and charged with 30 mL of THF, 6 mL of ethanol, 1.05 mL (10.0 mmol) of $^{i}Pr_2NH$, and 3.60 mL (27.5 mmol) of 2,4,6-collidine. A solution of 4.25 g (25.0 mmol) of $AgNO_3$ in dry CH_3CN was added in one portion and the mixture stirred vigorously for 24 h. The reaction was quenched by stirring with brine for 6 h, and the solids were filtered and rinsed with large portions of ether. The two layers of the filtrate were separated, and the organic layer was washed with water (3×) and brine and dried over Na_2SO_4. The solution was filtered, and the solvents were removed in vacuo. Low-boiling impurities were removed by vacuum distillation, and the dark yellow oil was used without further purification (1.64 g, 84% yield): ^{1}H NMR (400 MHz, $CDCl_3$) δ 0.89 (3H, t, J = 8 Hz), 1.78 (9H, t, J = 8 Hz), 1.26−1.35 (18H, comp), 1.62 (2H, m), 2.61, (2H, t, J = 8 Hz), 3.65 (6H, q, J = 8 Hz), 7.16 (2H, d, J = 8 Hz), 7.50 (2H, d, J = 8 Hz); ^{13}C NMR (100 MHz, $CDCl_3$) δ 14.3, 15.1, 22.8, 29.51, 29.52, 29.65, 29.74, 29.80, 29.81, 29.83, 31.5, 32.1, 35.9, 57.6, 114.0, 127.4, 128.0, 135.5, 143.4; HRMS (ESI) m/z calcd for $C_{25}H_{44}NaO_3$ 415.3183 [M + Na]$^+$, 415.3185.

2,6-Bis(4-dodecylphenyl)benzo[1,2-*d*;3,4-*d*′]bis(oxazole) (11). This compound was prepared and isolated analogously to BBO **9** from 0.11 g (0.50 mmol) of DAHQ, 0.63 g (1.60 mmol) of 4-dodecyl-1-(triethoxymethyl)benzene, and 43.5 mg of $Yb(OTf)_3$. The product was purified by recrystallization from THF to give white needles (0.21 g, 65% yield): mp >260 °C; ^{1}H NMR (400 MHz, $CDCl_3$) δ 0.90 (6H, t, J = 8 Hz), 1.28−1.37 (36H, comp 1.69 (4H, m), 2.71 (4H, t, J = 8 Hz), 7.35 (4H, d, J = 8 Hz), 7.89 (2H, s), 8.19 (4H, d, J = 8 Hz); ^{13}C NMR (100 MHz, $CDCl_3$) 14.2, 22.8, 29.48, 29.50, 29.6, 29.7, 29.81, 29.84, 31.3, 32.1, 36.3, 100.9, 124.9, 127.9, 129.2, 140.7, 147.4, 148.8, 164.7; HRMS (ESI) m/z calcd for $C_{44}H_{61}N_2O_2$ 649.4728 [M + H]$^+$, found 649.4730.

4,8-Dibromo-2,6-bis(4-dodecylphenyl)[1,2-*d*;3,4-*d*′]bis-(oxazole) (12). This compound was prepared and isolated analogously to BBO **10** from 0.15 g (0.50 mmol) of Br-DAHQ and 0.59 g (1.50 mmol) of 4-dodecyl-1-(triethoxymethyl)benzene, except the reaction mixture was heated to 65 °C. The product was purified by recrystallization from toluene (hot filter, charcoal) to give white needles (0.27 g, 68% yield): mp 154−156 °C; ^{1}H NMR (400 MHz, $CDCl_3$) δ 0.88 (6H, t, J = 8 Hz), 1.26−1.36 (36H, comp), 1.67 (4H, m), 2.70 (4H, t, J = 8 Hz), 7.35 (4H, d, J = 8 Hz), 8.25 (4H, d, J = 8 Hz); ^{13}C NMR (100 MHz, $CDCl_3$) δ 22.8, 29.46, 29.51, 29.6, 29.7, 29.8, 31.2, 32.1, 36.3, 91.8, 123.9, 128.3, 128.4, 129.2, 129.3, 139.9,

dx.doi.org/10.1021/jo4007927 | J. Org. Chem. XXXX, XXX, XXX−XXX

147.1, 148.2, 164.9; HRMS (APCI) m/z calcd for $C_{44}H_{59}Br_2N_2O_2$ 807.2918 $[M + H]^+$, found 807.2922.

4,8-Bis(4-dodecylphenyl)-2,6-bis(5-dodecylthien-2-yl)-benzo[1,2-*d*;3,4-*d*′]bis(oxazole) (13). This compound was prepared and isolated analogously to BBO 7 from BBO **10** (0.61g, 0.75 mmol) and (4-dodecylphenyl)boronic acid (0.54g, 1.88 mmol). The crude product was dissolved in $CHCl_3$ and passed through a pad of silica gel with $CHCl_3$ as eluent, and the solution was concentrated in vacuo. The product was further purified by recrystallization from $CHCl_3$ to give a bright yellow solid (0.72 g, 87% yield): mp 94−96 °C; ^{1}H NMR (400 MHz, $CDCl_3$) δ 0.91 (12H, comp), 1.29−1.46 (72H, comp), 1.74 (8H, comp), 2.75 (4H, t, J = 8 Hz), 2.88 (4H, t, J = 8 Hz), 6.85 (2H, d, J = 4 Hz), 7.43 (4H, d, J = 8 Hz), 7.76 (2H, d, J = 4 Hz), 8.29 (4H, d, J = 8 Hz); ^{13}C NMR (100 MHz, $CDCl_3$) δ 14.4, 22.92, 22.93, 29.3, 29.57, 29.58, 29.61, 29.75, 29.77, 29.84, 29.86, 29.89, 29.94, 29.95, 30.6, 31.68, 31.73, 32.14, 32.16, 36.2, 113.7, 125.6, 127.1, 128.8, 130.0, 130.3, 138.3, 143.2, 146.2, 152.1, 159.8; HRMS (ESI) m/z calcd for $C_{76}H_{113}N_2O_2S_2$ 1149.8238 $[M + H]^+$, found 1149.8229.

4,8-Bis(5-dodecylthien-2-yl)-2,6-bis(4-dodecylphenyl)[1,2-*d*;3,4-*d*′]bis(oxazole) (14). This compound was prepared and isolated analogously to BBO **8** from 0.32 g (0.40 mmol) of BBO **12** and 0.38 g (0.92 mmol) of 5-dodecyl-2-(trimethylstannyl)thiophene. The product was purified by recrystallization from ethyl acetate to give a yellowish orange powder (0.40 g, 87% yield): mp 97−100 °C; ^{1}H NMR (400 MHz, $CDCl_3$) δ 0.89 (12H, comp), 1.25−1.51 (72H, comp), 1.70 (4H, p, J = 8 Hz), 1.82 (4H, p, J = 8 Hz), 2.73 (4H, t, J = 8 Hz), 2.98 (4H, t, J = 8 Hz), 6.80 (2H, d, J = 3 Hz), 7.39 (4H, d, J = 8 Hz), 8.31 (4H, d, J = 8 Hz), 8.33 (2H, d, J = 4 Hz); ^{13}C NMR (100 MHz, $CDCl_3$) δ 14.2, 22.8, 29.44, 29.47, 29.52, 29.63, 29.68, 29.77, 29.83, 29.85, 29.9, 30.5, 31.3, 32.0, 32.1, 36.3, 108.1, 124.8, 124.9, 128.0, 129.1, 129.2, 132.2, 136.8, 144.6, 147.2, 148.2, 163.6; HRMS (APCI) m/z calcd for $C_{76}H_{113}N_2O_2S_2$ 1149.8238 $[M + H]^+$, found 1149.8259.

2,4,6,8-Tetrakis(5-dodecylthien-2-yl)[1,2-*d*;3,4-*d*′]bis-(oxazole) (15). This compound was prepared and isolated analogously to BBO **8** from 0.41 g (0.50 mmol) of BBO **10** and 0.47 g (1.13 mmol) of 5-dodecyl-2-(trimethylstannyl)thiophene. The product was purified by recrystallization from ethyl acetate to give a dark yellow powder (0.55 g, 94% yield): mp 78−80 °C; ^{1}H NMR (400 MHz, $CDCl_3$) δ 0.88 (12H, t, J = 8 Hz), 1.27−1.45 (72H, comp), 1.78 (8H, comp), 2.93 (8H, comp), 6.90 (2H, d, J = 4 Hz), 6.94 (2H, d, J = 4 Hz), 7.86 (2H, d, J = 4 Hz), 8.25 (2H, d, J = 4 Hz); ^{13}C NMR (100 MHz, $CDCl_3$) δ 14.3, 22.9, 29.26, 29.4, 29.5, 29.6, 29.7, 29.80, 29.82, 29.85, 30.4, 30.6, 31.7, 31.95, 32.08, 107.6, 124.8, 125.7, 127.0, 129.0, 130.4, 131.9, 136.5, 144.2, 148.2, 152.3, 159.4; HRMS (APCI) m/z calcd for $C_{72}H_{109}N_2O_2S_4$ 1161.7366 $[M + H]^+$, found 1161.7346.

2,4,6,8-Tetrakis(4-dodecylphenyl)[1,2-*d*:3,4-*d*′]bis(oxazole) (16). This compound was prepared and isolated similarly to 7 from 0.32 g (0.40 mmol) of **12** and 0.29 g (1.00 mmol) of 4-dodecylphenylboronic acid. The crude product was dissolved in $CHCl_3$ and passed through a pad of silica gel with $CHCl_3$ as eluent, and the solution was concentrated in vacuo. The product was purified by recrystallization from ethyl acetate to give white needles (0.34 g, 60% yield): mp 112−113 °C; ^{1}H NMR (400 MHz; $CDCl_3$) δ 0.89 (12H, comp), 1.27−1.45 (72H, comp), 1.64 (4H, m), 1.74 (4H, m), 2.68 (4H, t, J = 8 Hz), 2.75 (4H, t, J = 8 Hz), 7.31 (4H, d, J = 8 Hz), 7.44 (4H, d, J = 8 Hz), 8.21 (4H, d, J = 8 Hz), 8.35 (4H, d, J = 4 Hz); ^{13}C NMR (100 MHz; $CDCl_3$) δ 14.3, 22.85, 22.86, 29.45, 29.52, 29.54, 29.65, 29.69, 29.75, 29.78, 29.80, 29.82, 29.83, 29.9, 31.4, 31.6, 32.08, 32.10, 36.16, 36.21, 114.0, 124.8, 127.9, 128.8, 129.0, 130.1, 130.2, 138.4, 143.2, 146.4, 147.0; HRMS (APCI) m/z calcd for $C_{80}H_{117}N_2O_2$ 1137.9110 $[M + H]^+$, found 1137.9139.

Computational Details. All of the calculations on these oligomers studied in this work were carried out using Gaussian 03W with the GaussView 4 GUI interface program package. All electronic ground state geometries were optimized using density functional theory (DFT) employing an SVP functional and a 6-31G* basis set. All computations were performed using Gaussian 09 through the National Science Foundation's Extreme Science and Engineering Discovery Environment (XSEDE) and San Diego Supercomputer Center's Trestles Cluster. Excited states were generated through time-dependent density functional theory (TD-DFT) applied to the optimized ground state for each oligomer. The HOMO, LUMO, band gap, first 10 excited states, and UV−vis simulations were generated from these excited computations.

■ ASSOCIATED CONTENT

Ⓢ Supporting Information

Text, figures, and tables giving experimental procedures, ^{1}H and ^{13}C NMR spectra for new compounds, PL spectra of selected compounds, calculated atom coordinates, and absolute energies. This material is available free of charge via the Internet at http://pubs.acs.org.

■ AUTHOR INFORMATION

Corresponding Author

*E-mail for M.J.-E.: malikaj@iastate.edu.

Notes

The authors declare no competing financial interest.

■ ACKNOWLEDGMENTS

We acknowledge the donors of the Petroleum Research Fund for support of this work. We also thank the 3M Foundation and the National Science Foundation (DMR-0846607) for partial support of this work. We thank Kamel Harrata and the Mass Spectroscopy Laboratory Iowa State University (ISU) for analysis of our compounds. We thank Atta Gueye, Dr. Elena Sheina, and Dr. Christopher Brown of Plextronics for providing UPS measurements. We thank Scott Meester for the synthesis of 1-bromo-4-((3,7-dimethyloctyl)oxy)benzene. We also thank Dr. William Jenks (ISU), Dr. Jared Mike (Texas A&M University), and Dr. Jeremy Intemann (University of Washington) for helpful discussions on this research. We would like to thank the National Foundation Extreme Science Engineering Discovery Environment (TG-CHE120020) for providing the resources for all the computational work included in this article.

■ REFERENCES

(1) Horowitz, G. *Adv. Mater.* **1998**, *10*, 365.
(2) Mas-Torrent, M.; Rovira, C. *Chem. Soc. Rev.* **2008**, *37*, 827.
(3) Newman, C. R.; Frisbie, C. D.; daSilva Filho, D. A.; Bredas, J. L.; Ewbank, P. C.; Mann, K. R. *Chem. Mater.* **2004**, *16*, 4436.
(4) Murphy, A. R.; Frechet, J. M. J. *Chem. Rev.* **2007**, *107*, 1066.
(5) Dimitrakopoulos, C. D.; Malenfant, P. R. L. *Adv. Mater.* **2002**, *14*, 99.
(6) Tang, C. W.; VanSlyke, S. A. *Appl. Phys. Lett.* **1987**, *51*, 913.
(7) Veinot, J. G. C.; Marks, T. J. *Acc. Chem. Res.* **2005**, *38*, 632.
(8) Friend, R. H.; Gymer, R. W.; Holmes, A. B.; Burroughes, J. H.; Marks, R. N.; Taliani, C.; Bradley, D. D. C.; Dos Santos, D. A.; Bredas, J. L.; Logdlund, M.; Salaneck, W. R. *Nature* **1999**, *397*, 121.
(9) Alam, M. M.; Jenekhe, S. A. *Chem. Mater.* **2004**, *16*, 4647.
(10) Coakley, K. M.; McGehee, M. D. *Chem. Mater.* **2004**, *16*, 4533.
(11) Scharber, M.; Mühlbacher, D.; Koppe, M.; Denk, P.; Waldauf, C.; Heeger, A.; Brabec, C. *Adv. Mater.* **2006**, *18*, 789.
(12) Tang, C. W. *Appl. Phys. Lett.* **1986**, *48*, 183.
(13) Osowska, K.; Miljanic, O. S. *Chem. Commun.* **2010**, *46*, 4276.
(14) Lim, J.; Albright, T. A.; Martin, B. R.; Miljanić, O. Š. *J. Org. Chem.* **2011**, *76*, 10207.
(15) Klare, J. E.; Tulevski, G. S.; Sugo, K.; de Picciotto, A.; White, K. A.; Nuckolls, C. *J. Am. Chem. Soc.* **2003**, *125*, 6030.
(16) Wilson, J. N.; Josowicz, M.; Wang, Y.; Bunz, U. H. F. *Chem. Commun.* **2003**, 2962.
(17) Zucchero, A. J.; McGrier, P. L.; Bunz, U. H. F. *Acc. Chem. Res.* **2009**, *43*, 397.

(18) McGrier, P. L.; Solntsev, K. M.; Miao, S.; Tolbert, L. M.; Miranda, O. R.; Rotello, V. M.; Bunz, U. H. F. *Chem. -Eur. J* **2008**, *14*, 4503.
(19) Marsden, J. A.; Miller, J. J.; Shirtcliff, L. D.; Haley, M. M. *J. Am. Chem. Soc.* **2005**, *127*, 2464.
(20) Ohta, K.; Yamada, S.; Kamada, K.; Slepkov, A. D.; Hegmann, F. A.; Tykwinski, R. R.; Shirtcliff, L. D.; Haley, M. M.; Salek, P.; Gel'mukhanov, F.; Aagren, H. *J. Phys. Chem. A* **2011**, *115*, 105.
(21) Spitler, E. L.; Monson, J. M.; Haley, M. M. *J. Org. Chem.* **2008**, *73*, 2211.
(22) Spitler, E. L.; Shirtcliff, L. D.; Haley, M. M. *J. Org. Chem.* **2007**, *72*, 86.
(23) Kang, H.; Evmenenko, G.; Dutta, P.; Clays, K.; Song, K.; Marks, T. J. *J. Am. Chem. Soc.* **2006**, *128*, 6194.
(24) Tlach, B. C.; Tomlinson, A. e. L.; Bhuwalka, A.; Jeffries-EL, M. *J. Org. Chem.* **2011**, *76*, 8670.
(25) Intemann, J. J.; Hellerich, E. S.; Tlach, B. C.; Ewan, M. D.; Barnes, C. A.; Bhuwalka, A.; Cai, M.; Shinar, J.; Shinar, R.; Jeffries-EL, M. *Macromolecules* **2012**, *45*, 6888.
(26) Ripaud, E.; Olivier, Y.; Leriche, P.; Cornil, J. R. M.; Roncali, J. *J. Phys. Chem. B* **2011**, *115*, 9379.
(27) Wilson, J. N.; Windscheif, P. M.; Evans, U.; Myrick, M. L.; Bunz, U. H. F. *Macromolecules* **2002**, *35*, 8681.
(28) Klare, J. E.; Tulevski, G. S.; Nuckolls, C. *Langmuir* **2004**, *20*, 10068.
(29) May, J. C.; Biaggio, I.; Bures, F.; Diederich, F. *Appl. Phys. Lett.* **2007**, *90*, 251106.
(30) Gao, B.; Liu, Y.; Geng, Y.; Cheng, Y.; Wang, L.; Jing, X.; Wang, F. *Tetrahedron Lett.* **2009**, *50*, 1649.
(31) Würthner, F.; Thalacker, C.; Diele, S.; Tschierske, C. *Chem. Eur. J.* **2001**, *7*, 2245.
(32) Wilson, J. N.; Hardcastle, K. I.; Josowicz, M.; Bunz, U. H. F. *Tetrahedron* **2004**, *60*, 7157.
(33) Hegedus, L. S.; Odle, R. R.; Winton, P. M.; Weider, P. R. *J. Org. Chem.* **1982**, *47*, 2607.
(34) Mike, J. F.; Inteman, J. J.; Ellern, A.; Jeffries-EL, M. *J. Org. Chem.* **2010**, *75*, 495.
(35) Mike, J. F.; Makowski, A. J.; Jeffries-EL, M. *Org. Lett.* **2008**, *10*, 4915.
(36) Mike, J. F.; Intemann, J. J.; Cai, M.; Xiao, T.; Shinar, R.; Shinar, J.; Jeffries-EL, M. *Polym. Chem.* **2011**, *2*, 2299.
(37) Brown, R. D.; Buchanan, A. S.; Humffray, A. A. *Aust. J. Chem.* **1965**, *18*, 1521.
(38) Tschitschibabin, A. E. *Ber. Bunsen-Ges. Phys. Chem.* **1905**, *38*, 561.
(39) Breslow, R.; Pandey, P. S. *J. Org. Chem.* **1980**, *45*, 740.
(40) Mamane, V.; Aubert, E.; Fort, Y. *J. Org. Chem.* **2007**, *72*, 7294.
(41) Bhuwalka, A.; Mike, J. F.; He, M.; Intemann, J. J.; Nelson, T.; Ewan, M. D.; Roggers, R. A.; Lin, Z.; Jeffries-EL, M. *Macromolecules* **2011**, *44*, 9611.
(42) Salaneck, W. R. *J. Electron Spectrosc. Relat. Phenom.* **2009**, *174*, 3.
(43) Miyamae, T.; Yoshimura, D.; Ishii, H.; Ouchi, Y.; Miyazaki, T.; Koike, T.; Yamamoto, T.; Muramatsu, Y.; Etori, H.; Maruyama, T.; Seki, K. *Synth. Met.* **1997**, *84*, 939.
(44) Lois, S.; Florès, J.-C.; Lère-Porte, J.-P.; Serein-Spirau, F.; Moreau, J. J. E.; Miqueu, K.; Sotiropoulos, J.-M.; Baylère, P.; Tillard, M.; Belin, C. *Eur. J. Org. Chem.* **2007**, *2007*, 4019.
(45) Nijegorodov, N. I.; Downey, W. S. *J. Phys. Chem.* **1994**, *98*, 5639.
(46) Berlman, I. B. *J. Phys. Chem.* **1970**, *74*, 3085.
(47) Huang, W.; Yin, J. *Polym. Eng. Sci.* **2007**, *47*, 429.
(48) *Principles and Applications of Photochemistry*; Wiley: Hoboken, NJ, 2009.
(49) Dollish, F. R.; Fateley, W. G.; Bentley, F. F. *Characteristic Raman Frequencies of Organic Compounds*; Wiley-Interscience: New York, 1973.
(50) So, Y.-H.; Zaleski, J. M.; Murlick, C.; Ellaboudy, A. *Macromolecules* **1996**, *29*, 2783.
(51) Caspar, J. V.; Meyer, T. J. *J. Phys. Chem.* **1983**, *87*, 952.
(52) Tolbert, L. M.; Nesselroth, S. M.; Netzel, T. L.; Raya, N.; Stapleton, M. *J. Phys. Chem.* **1992**, *96*, 4492.
(53) Zucchero, A. J.; Wilson, J. N.; Bunz, U. H. F. *J. Am. Chem. Soc.* **2006**, *128*, 11872.
(54) Zhang, H. C.; Guo, E. Q.; Zhang, Y. L.; Ren, P. H.; Yang, W. J. *Chem. Mater.* **2009**, *21*, 5125.
(55) Chase, D. T.; Young, B. S.; Haley, M. M. *J. Org. Chem.* **2011**, *76*, 4043.
(56) Pak, J. J.; Weakley, T. J. R.; Haley, M. M. *J. Am. Chem. Soc.* **1999**, *121*, 8182.
(57) Melhuish, W. H. *J. Phys. Chem.* **1961**, *65*, 229.
(58) Tlach, B. C.; Tomlinson, A. L.; Bhuwalka, A.; Jeffries-EL, M. *J. Org. Chem.* **2011**, *76*, 8670.
(59) Bo, Z.; Schlüter, A. D. *J. Org. Chem.* **2002**, *67*, 5327.
(60) Kannan, R.; He, G. S.; Lin, T.-C.; Prasad, P. N.; Vaia, R. A.; Tan, L.-S. *Chem. Mater.* **2003**, *16*, 185.
(61) Wang, X.; Ng, J. K.-P.; Jia, P.; Lin, T.; Cho, C. M.; Xu, J.; Lu, X.; He, C. *Macromolecules* **2009**, *42*, 5534.
(62) Saikia, G.; Iyer, P. K. *J. Org. Chem.* **2010**, *75*, 2714.
(63) Zysman-Colman, E.; Arias, K.; Siegel, J. S. *Can. J. Chem.* **2009**, *87*, 440.
(64) Leermann, T.; Leroux, F. R.; Colobert, F. *Org. Lett.* **2011**, *13*, 4479.
(65) Yoon, M.-H.; DiBenedetto, S. A.; Facchetti, A.; Marks, T. J. *J. Am. Chem. Soc.* **2005**, *127*, 1348.
(66) Kim, J.-J.; Lim, K.; Choi, H.; Fan, S.; Kang, M.-S.; Gao, G.; Kang, H. S.; Ko, J. *Inorg. Chem.* **2010**, *49*, 8351.
(67) Ellinger, S.; Kreyes, A.; Ziener, U.; Hoffmann-Richter, C.; Landfester, K.; Möller, M. *Eur. J. Org. Chem.* **2007**, *2007*, 5686.
(68) Firouzabadi, H.; Iranpoor, N.; Hazarkhani, H. *J. Org. Chem.* **2001**, *66*, 7527.